The Response of both Surface Reflectance and the Underwater Light Field to Various Levels of Suspended Sediments: Preliminary Results

Luoheng Han and Donald C. Rundquist

Abstract

The purpose of the research was to investigate the relationships between and among surface spectral reflectance, the underwater light field, and suspended sediment concentrations (SSC). Both spectroradiometer and quantum-sensor data were collected over and in an 8543 litre vinyl pool, under natural sunlight. Twenty levels of SSCs ranging from 50 to 1000 mg/l were put into solution. Both downwelling and upwelling irradiances below the water surface decreased with increasing SSC, even though atmospheric downwelling increased. A relationship for PAR (Photosynthetically Active Radiation) transmittance, reflectance, and absorption with varying levels of SSC was illustrated. The association between surface spectral reflectance and SSC was linear at low levels and non-linear at high level of SSC. Specific spectral locations of peak reflectance with varying SSC were documented. First derivatives of peak reflectance, at 823.3 nm, correlated more highly with SSC than peak reflectance itself.

Introduction

The quality of water in streams, lakes, and reservoirs is an environmental concern of global proportions (Ritchie *et al.*, 1990). One important water-quality issue is the degradation of these surface waters by suspended particulate materials originating from soil erosion and associated overland run-off (Brown, 1984).

The remote measurement of surface water quality is appealing to resource managers because it offers not only multi-temporal spatial data but also a synoptic view that is unmatched by surface data-collection techniques (Alföldi, 1982). One other important advantage of remote sensing of water bodies is the integrated response, or "area-averaging," which occurs in the measurement procedure. This integrated signal is useful for water quality because the analyst usually is interested in characterizing an entire lake, or large portions of individual water bodies.

Purpose of Study

The purpose of our study is to investigate the relationships between and among surface spectral reflectance, the underwater light field, and suspended sediment concentrations (SSC). The work summarized in this paper differs from previous works in the following ways: (1) we chose to collect our data in natural sunlight, as opposed to more commonly used artificial-light sources; (2) the water container used in our work is considerably larger than those normally used; (3) we included measurements and analyses of the underwater light field, a phenomenon which tends to be omitted in most published works; and (4) we attempted to determine precise levels of SSC that are required to produce specific types of spectral responses at the water surface.

Literature Review

Satellite Remote Sensing of SSC

A great deal of work has been carried out on the measurement of SSC using satellite remote sensing data, especially from the Landsat Multispectral Scanner (MSS) and Thematic Mapper (TM). Alfldi and Munday (1978) applied the chromaticity concept to the problem of discriminating suspended solids, as well as certain other water quality parameters. Munday and Alfldi (1979) also used Landsat MSS data to test diffuse-reflectance models for measuring aquatic suspended solids. Khorram and Cheshire (1985) used Landsat MSS digital data combined with surface measurements of water quality (including suspended solids) to map conditions in the Neuse River Estuary, North Carolina. Aranuvachapun and Walling (1988) examined Landsat MSS radiance data for estimating SSC in the Lower Yellow River (Hwang Ho), China. Lyon *et al.* (1988) processed multitemporal Landsat and AVHRR data to determine SSC in Sandusky Bay, Lake Erie. Doerffer *et al.* (1989) analyzed Landsat TM data with respect to its capability for mapping the complex structure and dynamics of suspended-matter distribution in the coastal area of the German Bight (North Sea). Jensen *et al.* (1989) attempted to model salinity and suspended-sediment distributions in Laguna de Terminus, Mexico, using Landsat TM data. Ritchie *et al.* (1990) compared six concurrent Landsat MSS and TM scenes to relate Landsat digital data to suspended sediments, chlorophyll, and temperature in the surface water of Moon Lake, Mississippi. Schiebe *et al.* (1992) evaluated several possible models linking Landsat MSS data and measurements of SSC in Lake Chicot, Arkansas. SPOT data have been used for similar studies (e.g., Lathrop and Lillesand, 1990). The relationship between SSC and remotely

Center for Advanced Land Management Information Technologies, Conservation and Survey Division, University of Nebraska – Lincoln, Lincoln, NE 68588-0517.

L. Han is presently with the Department of Geography, The University of Alabama, 202, Farrah Hall, Box 870322, Tuscaloosa, AL 35487-0322.

TABLE 1. WEATHER CONDITIONS DURING DATA COLLECTION

Date	Time	Air Temp. (F)	Rel Hum. (%)	Wind Sp. (m s¹)	Wind Dir. (Degrees)	Solar (W m²)
6/25	1100	81.82	54.73	4.66	331.80	795.00
6/25	1200	83.25	45.95	5.78	338.60	904.00

sensed spectral radiance was also reviewed by Curran and Novo (1988).

Although satellite remote sensing is a proven technique for monitoring and analyzing water bodies affected by suspended materials, the application of the technology to studies of fresh water has been limited mainly by the coarser spatial and spectral resolution of easily available data. In addition, most available satellite sensors with suitable resolution were designed with land surveys in mind. Therefore, the number of spectral channels, their distribution, and the range of brightness have not been optimized for water (Hilton, 1984).

Close-Range Hyperspectral Remote Sensing of SSC
The remote sensing of surface waters may be complicated by a number of extraneous variables, including atmospheric attenuation, angle of illumination, angle of observation, surface roughness, and bottom effects (Campbell, 1987). Therefore, the researcher may choose to conduct experiments at close range in order to either control or exclude one or more of the confounding variables. In addition, by using a "hyperspectral" remote sensing system, which acquires data in more than 100 channels, one should be able to accurately characterize the volume reflectance of the water body and thereby infer the SSC in the water.

Several investigators have analyzed the relationship between SSC and remotely acquired measures of reflectance using "hyperspectral" instruments at close range. Novo et al. (1989a) measured, using a spectroradiometer, the reflectance of pure water in the laboratory and compared it to four concentrations of white clay and red silt. It was concluded that sediment type can affect the strength of the correlation between SSC and reflectance, especially at short wavelengths. Bhargava and Mariam (1990) studied the spectral response of turbid waters caused by different clay materials. The analysis showed a linear relationship between turbidity and percentage reflectance for bentonite clay and black cotton soil, whereas curvilinear variation was observed for kaoline and gray soil. Novo et al. (1991) conducted a laboratory experiment to determine the optimal wavelengths for estimating of total suspended solids (TSS). They found that, for oxisoil sediment, there was a linear correlation between spectral reflectance and TSS concentration. The correlation was statistically significant and constant from 450 to 900 nm, but the peak spectral reflectance with high TSS concentration occurred in the red region of the spectrum. Mantovani and Cabral (1992) studied the optimum tank depth for the assessment of spectral reflectance from suspended inorganic matter. Different concentrations of bentonite and red silt suspensions were produced and radiometric measurements were performed in the 400- to 900-nm spectral range. The results showed that the optimum depth for measuring SSC is dependent on the type of soil in suspension. Other related works include Ritchie et al. (1976), Moore (1978), Mckim et al. (1984), Bukata et al. (1985), Vertucci and Likens (1989), Quibell (1991), Bukata et al. (1991), and Dekker et al. (1992).

The generally documented evidence for remote sensing of SSC includes (1) reflectance increases with increasing SSC (Ritchie et al., 1976; Moore, 1978; McKim et al., 1984); (2) the peak reflectance shifts to longer wavelengths with increasing concentrations (Alföldi, 1982); and (3) the relationship between SSC and spectra is dependent on the properties of sediments, the wavelength and viewing angle of the sensor, and the depth of the bottom (Bartolucci et al., 1977; Novo et al., 1989a; Novo et al., 1989b; Bhargava and Mariam, 1990; Mantovani and Cabral, 1992).

Experimental Design

Study Site and Sky Conditions During Data Collection
Our experiment was conducted at the Mead Research and Development Center (96°25'51" W and 41°10'34" N), an agricultural research station of the University of Nebraska-Lincoln, on 25 June 1992, under clear skies (see pertinent conditions in Table 1). All data collection occurred between 11 AM and noon, local daylight saving time. Because the measurements were close to solar noon, variability in solar elevation was minimized and solar illumination was maximized (as per Deering (1989)).

The Water Container
The water tank used for the experiment was an 8543-litre vinyl pool, 366 cm in diameter and 91 cm in depth. The walls and bottom of the pool were lined with black plastic to eliminate extraneous internal reflectances (McCluney, 1976). The pool was filled with clear well water to 80 cm, so the total volume of water for our work was 7510 litres. The pool was located in an open field at the Mead site.

Measurements Related to Underwater Light Fields
For measurements involving underwater light fields, two Li-Cor* (Li-192SA) Underwater Quantum Sensors were placed at a depth of 50 cm from the surface, with one facing upward to measure the downwelling irradiance beneath the surface and the other facing downward to measure the upwelling irradiance (Figure 1). The quantum instruments, which record amounts of photosynthetically active radiation (PAR — 400 to 700 nm) in the water, measure photosynthetic photon flux density (PPFD) in micromoles per second per metre squared (μmol s¹ m²). One Li-Cor (Li-190SA) Terrestrial Quantum Sensor was positioned 309 cm above the water level, clear of obstacles, to measure the total downwelling PAR incident on the surface of the pool (Figure 1).

Instrumentation for Measuring Surface Spectral Reflectance
A Spectron Engineering SE-590 spectroradiometer was used to collect radiance upwelling from the pool. This instrument acquires data in 256 discrete channels, among which 252 are used for recording radiance with four reserved for file-header information. The spectral range of the instrument is from 368.4 to 1113.7 nm. For our study, data from 402.1 to 896.4 nm (170 channels) were used because of significant noise in the water signal at wavelengths shorter than 400 nm and longer than 900 nm. The instrument consists basically of two components: head and controller. The instrument head was attached to a telescoping, truck-mounted boom. The boom was pointed south with the truck oriented east-west. The Spectron sensor was positioned over the center of the pool at

---

*Any use of trade names and/or trademarks in this publication is for descriptive purposes only and does not constitute endorsement by The University of Nebraska.
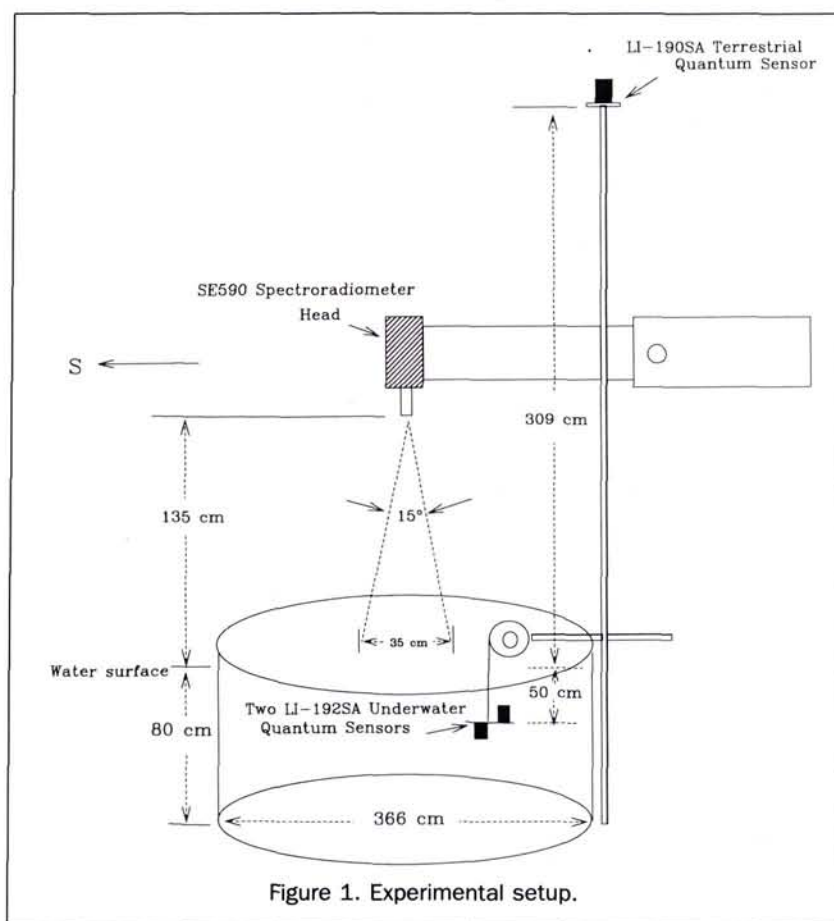
Figure 1. Experimental setup.

a height of 135 cm (Figure 1). A nadir view angle was se-lected for use (Novo *et al.*, 1989b). The 15° optic resulted in an instantaneous field of view of 35 cm by 35 cm on the wa-ter surface (Figure 1). The controller was connected to a mi-crocomputer, which initiated spectroradiometer scanning and stored the data. A Barium-Sulfate ($BaSO_4$) reference panel (70 cm by 70 cm) served as the calibration standard. Bi-direc-tional reflectance factors ($R(\lambda)$, in percent) were calculated using the following equation:

$$R(\lambda) = \frac{L(\lambda)}{S(\lambda)} Cal(\lambda) \times 100 \qquad (1)$$

where $L(\lambda)$ is the wavelength-specific target radiance, $S(\lambda)$ is the corresponding radiance from the $BaSO_4$ reference panel, and $Cal(\lambda)$ is the calibration factor for the $BaSO_4$ panel. The latter allowed correction both for the non-Lambertian proper-ties of the panel and the slight changes in solar-zenith angle. Two replicate scans were taken for each sample and the mean of the two was used in the analyses.

The Suspended Material

A clay loam soil was chosen for use as suspended matter in the experiment because it was readily available at the re-search site (Table 2). The samples were dried, sieved, and placed in plastic bottles. Each bottle contained 375 grams of the dry sample, or 50 mg/l of SSC in a volume of 7510 litres of water. A total of 20 samples were used for the experiment. The soil sediments were kept in suspension in the large wa-

TABLE 2. PHYSICAL PROPERTIES OF THE SOIL SEDIMENT USED

Percent Sand	Percent Coarse Silt	Percent Fine Silt	Percent Very Fine Silt	Percent Clay	Organic Matter (%)	Texture Class	Color
31.19	0.53	26.57	13.29	28.42	2.37	Clay Loam	10 YR 5/6

ter tank by manually stirring at regular intervals. The pool was scanned with the spectroradiometer within 20 seconds of sediment addition in order to minimize the amount of ma-terial settling to the bottom.

Results and Discussion

Measurements Pertaining to the Underwater Light Field

Measurements of terrestrial and underwater PAR fluxes were taken at 4- to 6-minute intervals, concurrent with spectrora-diometer scans (Table 3). The atmospheric downwelling irra-diance (E_{do}), the sum of direct solar and diffuse sky radiation, tended to increase as solar noon approached (Ta-ble 3), which is not surprising given the start and end times for the experiment. Minor fluctuations in the incoming PAR occurred at 1128, between 1148 and 1152, and at 1219 hours.

The second parameter measured was underwater down-welling irradiance (E_d) at 50 cm below the surface of the wa-

TABLE 3. RADIATION (PAR) MEASUREMENTS AND CALCULATIONS

Time of Day	SSC (mg/l)	Downwelling $(E_{do})^*$ at surface	Downwelling $(E_d)^*$ at 50 cm	Upwelling $(E_u)^*$ at 50 cm	k	R	Et (E_d/E_{do})	Er $(R^*E_{do}-E_u)/E_{do}$	Ea $(100-Et-Er)$
1056	0	1665	1278	36.4	0.23	1.26	76.76	−0.92	23.24
1100	50	1685	726.8	31.33	0.73	2.25	43.12	0.39	56.49
1104	100	1698	626.1	21.72	0.87	2.67	36.87	1.39	61.74
1110	150	1706	517.4	14.89	1.04	3.06	30.33	2.77	66.9
1114	200	1735	459.2	14.39	1.15	3.14	26.47	2.31	71.22
1118	250	1763	440.8	17.52	1.21	3.12	25	2.12	72.88
1122	300	1789	355.6	15.45	1.4	3.30	19.88	2.44	77.68
1128	350	1781	305	9.36	1.53	3.38	17.13	2.85	80.02
1132	400	1809	243	8.65	1.74	3.46	13.43	2.97	83.6
1136	450	1809	205.1	6.21	1.89	3.60	11.34	3.25	85.41
1139	500	1837	168.8	4.62	2.07	3.56	9.19	3.31	87.5
1145	550	1904	156.5	4.88	2.17	3.77	8.23	3.52	88.25
1148	600	1841	123	3.84	2.35	4.37	6.68	4.16	89.16
1152	650	1831	101.8	2.78	2.51	4.20	5.56	4.04	90.4
1157	700	1907	81.5	2.48	2.74	3.99	4.27	3.86	91.87
1207	750	1908	90.14	3.08	2.65	3.93	4.72	3.77	91.51
1211	800	1916	77.84	2.33	2.78	3.93	4.06	3.8	92.14
1216	850	1924	75.22	1.79	2.82	3.99	3.91	3.9	92.19
1219	900	1904	56.92	1.47	3.05	4.03	2.99	3.95	93.06
1223	950	1932	44.41	1.23	3.27	4.28	2.3	4.21	93.49
1226	1000	1944	41.52	0.94	3.34	4.18	2.14	4.13	93.73

The unit of measurement is $\mu mol\ s^1\ m^2$

ter (Table 3). Not surprisingly, E_d decreased as SSC increased. The only anomalous E_d reading occurred at 1157 hours. Notice that, because of increasing SSC, increasing E_{do} had little or no observable impact on E_d. We believe that the exact nature of this interrelationship is deserving of further research.

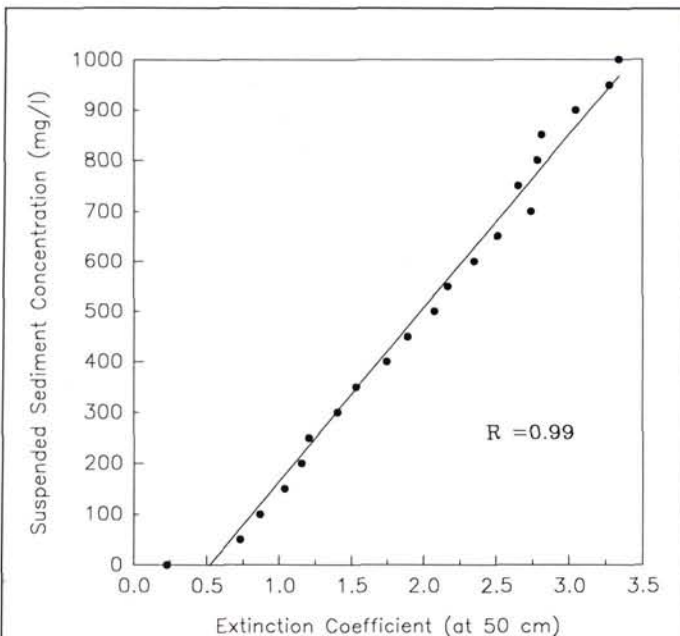Upwelling irradiance (E_u) from the tank bottom and water column beneath 50 cm was also measured concurrent with spectroradiometer scanning. E_u is a complex parameter because it should be dependent on the total radiation incident to the surface (E_{do}), SSC in the top 50 cm of the water, SSC below the 50-cm measurement point, and any reflective effect of the bottom itself. Like E_d, E_u decreased with increased SSC, again despite increasing E_{do} during that period. Minor irregularities in the pattern of decreasing E_u occurred at 1118, 1122, 1145, and 1207 hours. These findings demonstrate that the absorption and scattering caused by suspended sediments are important controls in the underwater light field. Notice that the actual rate of decrease in both E_d and E_u decreased as SSC increased, which highlights some nonlinearity in the relationship between SSC and certain components of the underwater light field.

The vertical extinction coefficient (k) quantifies the "quenching" of light as it passes from the water surface to the quantum sensor at 50 cm. Extinction coefficients are expressed as

$$E_d = E_{do}e^{-kz} \qquad (2)$$

which describes the amount of light remaining, E_d, after passing through water with a thickness of 0.5 metres, z. The original light intensity at zero depth was E_{do}.

Rearranging, we obtain

$$k = \frac{\log E_{do} - \log E_d}{z} \qquad (3)$$

The data in Table 3 show a trend of increasing k, except at 1207 hours. For clear water (SSC= 0 mg/l), k was 0.23, while for turbid water (SSC=1000 mg/l), k was 3.34. Figure 2 documents the expected positive relationship between SSC and k. For the soil used in our experiment, SSCs can be estimated by extinction coefficients using a linear regression model of the form

$$SSC(mg/l) = -178.5 + 342.9k \qquad (4)$$

The strong relationship exhibited and the model itself are

Figure 2. Relationship between SSC and extinction coefficient.
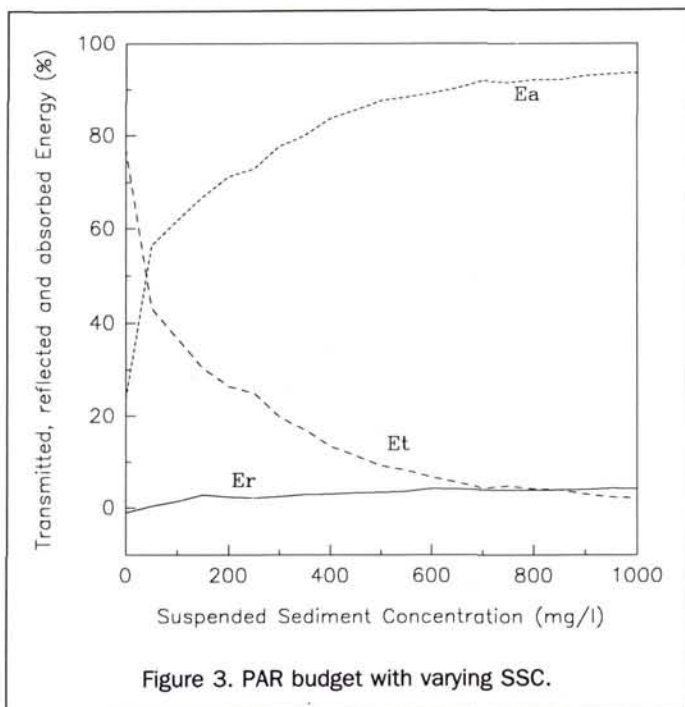
Figure 3. PAR budget with varying SSC.

important because the level of turbidity of a water body can be measured by means of computing k, instead of measuring SSC. From a practical standpoint, this may be useful in situations where underwater photometric equipment is available but sampling and laboratory analyses are not.

The R data in Table 3 were accumulated by integrating 107 channels (from 402.1 to 702.2 nm) of spectroradiometer data. Thus, we use R to represent PAR reflectance from the water surface. Notice that R tended to increase as SSC increased, with a few minor exceptions.

The measurements of E_{do}, E_d, E_u, and R, in conjunction with variable SSC, allowed us to examine the energy budget for PAR in the top 50 cm of water. As is commonly known, when electromagnetic energy reaches the surface of a water body, it may be reflected, absorbed, or transmitted (Lillesand and Kiefer, 1987). Thus, the interrelationship among these three processes can be expressed as

$$Ei = Et + Er + Ea \qquad (5)$$

where Ei is incident energy (E_{do}, in our case); Et is transmitted energy (E_d/E_{do}); Er is reflected energy ($(R*E_{do} - E_u)/E_{do}$ or $R - E_u/E_{do}$); and Ea is absorbed energy ($100 - Et - Er$).

The interrelationship involving PAR transmittance, reflectance, and absorption (in percent) with increasing SSC is shown as Figure 3. Notice that, as SSC increased from 0 to 1000 mg/l, absorption increased from 23 percent to nearly 94 percent (see also Table 3). Transmittance behaved oppositely, decreasing from 77 percent to about 2 percent. The biggest rate of increase in absorption and the biggest rate of decrease in transmittance occurred between 0 mg/l (clear water) and 50 mg/l of SSC. From 50 to 300 mg/l, the absorption increased about 21 percent (56.49 percent to 77.68 percent) while transmittance decreased about 23 percent (43.12 percent to 19.88 percent). From 300 to 600 mg/l, the increase in absorption was only about 11 percent (77.68 percent to 89.16 percent) while transmittance decreased only 13 percent

(19.88 percent to 6.68 percent). Above 600 mg/l, the changes in both were less than 5 percent. From 0 mg/l to 1000 mg/l of SSC, reflectance increased only about 4 percent (−0.92 percent to 4.21 percent) (Table 3). For clear water, the negative reflectance value (−0.92 percent) indicated that no PAR energy was upwelling in the top 50 cm of the water body, and in fact, the balance was negative, presumably due either to a large amount of absorption or sensor noise.

Surface Spectral Reflectance with Varying SSCs

Results of spectroradiometer data collection are summarized graphically as Figure 4. As SSC increased from 50 to 300 mg/l, the reflectance increased uniformly, for the most part, at wavelengths between 575 and 900 nm (Figure 4a). However, at wavelengths shorter than 575 nm, visual separation of spectral curves is more difficult. From 350 to 600 mg/l, the spectral profiles became somewhat irregular (e.g., at 450 mg/l and 500 mg/l), suggesting that the relationship was becoming non-linear (Figure 4b). At levels of 650 mg/l SSC and above, the spectra were virtually indistinguishable, for the most part (Figure 4c).

A simple linear regression model was used to estimate SSC based on spectral reflectance. The model can be expressed as

$$SSC(mg/l) = a + bX \qquad (6)$$

where X is spectral reflectance of a selected spectroradiometer channel, and a, b are regression coefficients. Based on this model, the correlation coefficient (per channel) was calculated to summarize the relationship between SSC and reflectance. Thus, a total of 170 correlation coefficients were computed. Results ranged from 0.21 to 0.97. Figure 5 indicates that the correlation coefficients were greater than 0.9 at wavelengths between 700 and 900 nm, and greater than 0.95 at wavelengths between 726 and 868 nm.
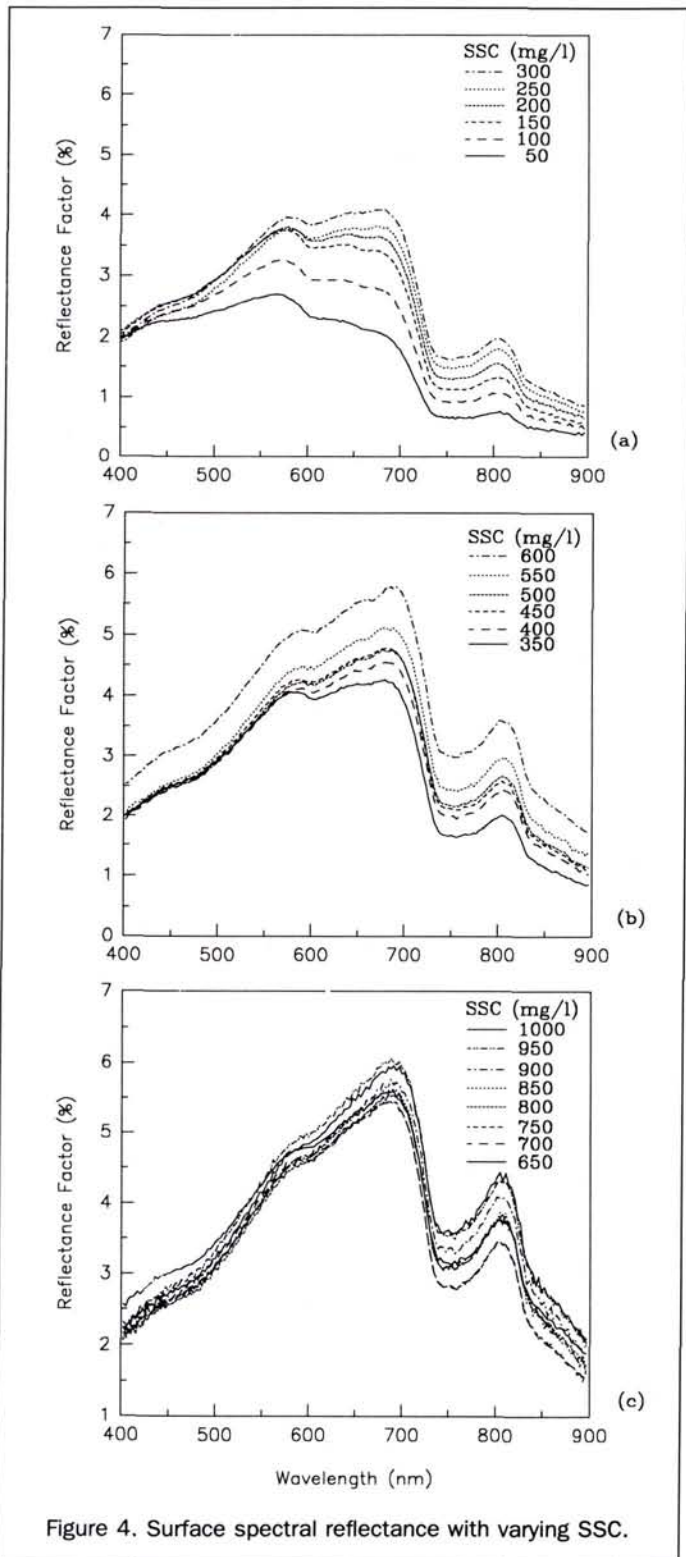
To investigate possible residuals from the linear regression model, the wavelength of 801.3 nm, at which the highest correlation (0.97) between SSC and reflectance occurred, was examined in detail. Figure 6 shows that errors from the model estimates exist above 600 mg/l of SSC. A total of five points were outside the 95 percent confidence interval, shown by the lines. This evidence may suggest that one should be cautious in using a linear regression model for estimating SSC from spectral reflectance at suspensions above 600 mg/l.

The wavelengths of the peak reflectance were plotted against SSCs (Figure 7). As expected, peak reflectance occurred at short visible wavelengths when SSC was low, but occurred at longer wavelengths when SSC was high. From 50 to 200 mg/l, the peak reflectance occurred around 575 nm with only minor differences. When SSC reached 250 mg/l, the peak reflectance shifted to 675 nm and increased only slightly with increased sediment loading.
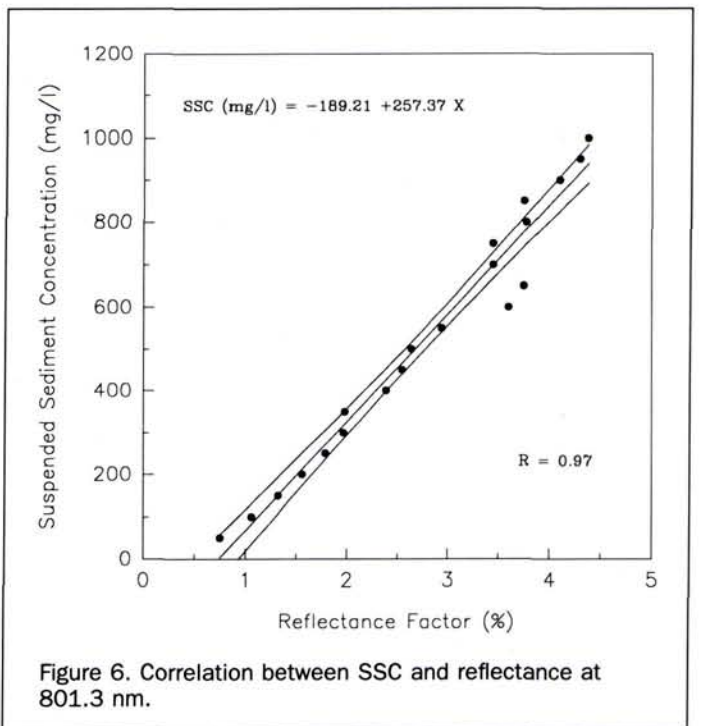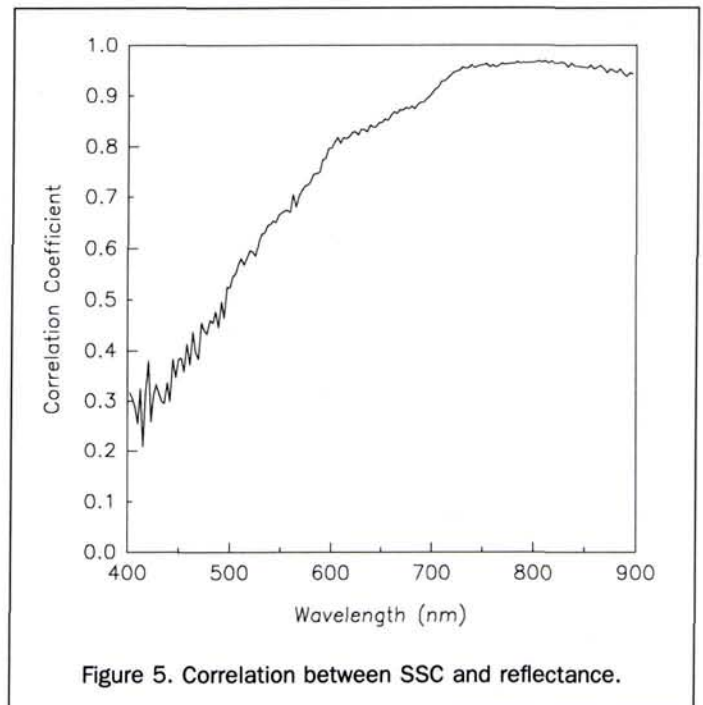
Correlation coefficients were also computed to describe the relationship between SSC and k. Correlations were greater than 0.9 at wavelengths between 685 and 900 nm (Figure 8). This result, along with what was described above, agrees with other researchers (for example, Bhargava and Mariam (1990), who demonstrated that 700 to 900 nm was the optimal wavelength range for measuring SSC).
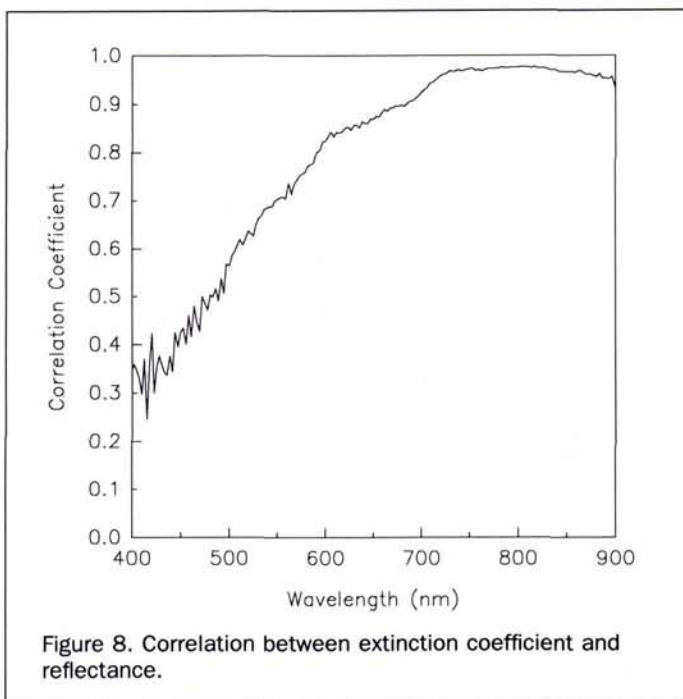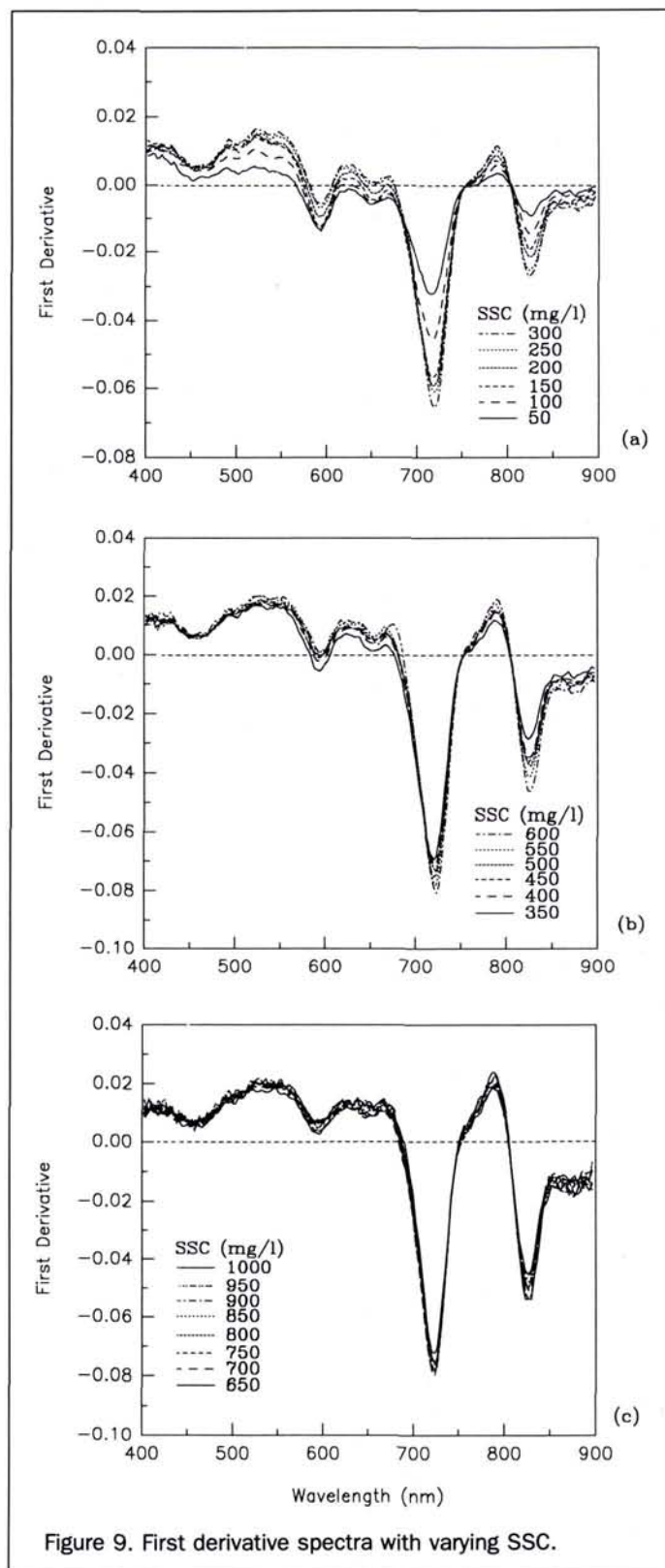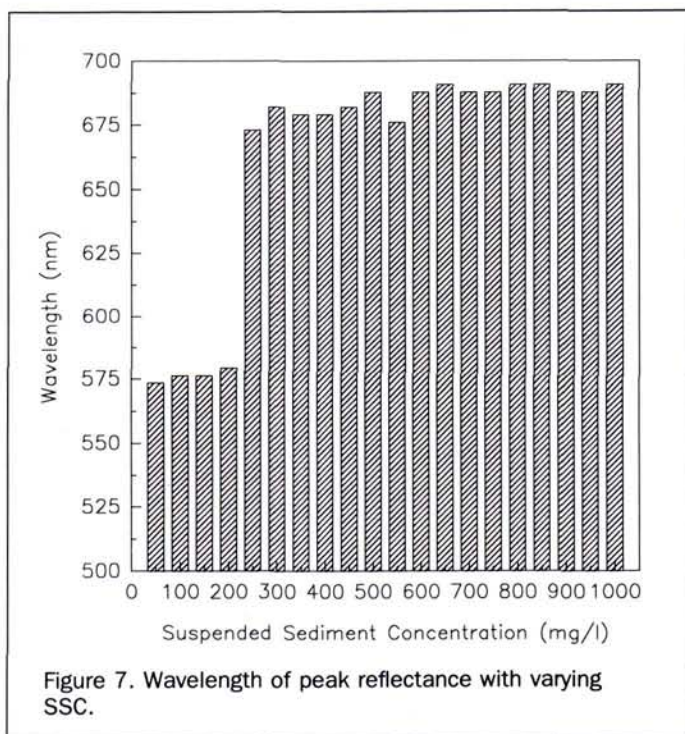
Derivative Spectra

The first derivative of a spectral reflectance can be defined as its rate of change with respect to wavelength (dy/dx). We

Figure 4. Surface spectral reflectance with varying SSC.

Figure 5. Correlation between SSC and reflectance.

Figure 6. Correlation between SSC and reflectance at 801.3 nm.

computed derivatives for the spectroradiometer data in hopes of elucidating further the SSC and reflectance relationship. The derivatives were computed by dividing the difference between successive reflectance values by the wavelength in-

terval separating them (Demetriades-Shah *et al.*, 1990), after applying a seven-point smoothing filter. Results are summarized in Figure 9. When SSCs are between 50 and 300 mg/l, the derivative spectra seem visually separable with the greatest separation occurring at about 720, 775, and 820 nm (Figure 9a). The slopes of reflectance spectra increased as SSC

Figure 7. Wavelength of peak reflectance with varying SSC.

Figure 8. Correlation between extinction coefficient and reflectance.

increased, at most wavelengths. From 350 to 600 mg/l, the derivative spectra appear less separable (Figure 9b). Above 650 mg/l, the curves are virtually identical (Figure 9c). In general, derivatives tended to be positive for visible wavelengths and negative for near-infrared wavelengths.

The relationship between first derivatives and SSC was

Figure 9. First derivative spectra with varying SSC.

TABLE 4. COMPARISON OF EQUATIONS 6 AND 7sm

Regression Model	R	Standard Error of Estimate
Derivative	0.99	1437.62
Reflectance	0.97	3018.62

examined by means of regression. We determined that SSC can be estimated using a second-order model of the form

$$SSC(mg/l) = a + b\chi + c\chi^2 \qquad (7)$$

χ where is the derivative of reflectance for selected channels, and a, b, and c are regression coefficients.

To evaluate the model linking SSC and first derivatives (Equation 7) and the model linking SSC and reflectance (Equation 6), the channels with the highest correlations (823.3 nm for derivative spectra and 801.3 nm for reflectance) were compared (Table 4). Notice that the model based on the first derivatives of reflectance at 823.3 nm (Equation 7) outperformed the model based on simple reflectance at 801.3 (Equation 6). The higher correlation coefficient and lower standard error attest to this fact. In addition, the plotted data (Figure 10) reveal a very good fit, especially at concentrations above 650 mg/l (compare to Figure 6).

Summary and Conclusions

The useful findings from the research included (1) as the suspended sediment concentration increased, there was a relatively small increase in reflected energy compared to a large increase in energy absorbed; (2) the non-linearity of the relationship between SSC and surface spectral reflectance appeared as SSC reached 350 mg/l, and at 650 mg/l and above, spectral curves were indistinguishable; (3) 700 to 900 nm

was the optimal wavelength range for measuring SSC; (4) the wavelength of peak reflectance shifted from 575 to 675 nm as SSC increased to 250 mg/l; and (5) the first derivative was effective in estimating SSC.

The research summarized in this paper leads us to continue our advocacy of both hyperspectral remote sensing at close range and controlled experimentation to establish and/or substantiate concepts related to suspended sediments. We support collecting spectral data in natural sunlight to facilitate linkages with remote sensing by aircraft and/or satellites. The use of large tanks of water with sufficient path lengths for light provides for a measure of reality, and we believe the inclusion of data collected underwater leads to an improved understanding of surface spectra. We expect studies such as ours, which focus on details of the remote-sensing/water-quality relationship, to have special relevance to analysis of data from future sensors with improved spectral resolutions.

References

Aranuvachapun, S., and D.E. Walling, 1988. Landsat-MSS radiance as a measure of suspended sediment in the Lower Yellow River (Hwang Ho), *Remote Sensing of Environment*, 25:145-165.

Alföldi, T.T., 1982. Remote sensing for water quality monitoring, *Remote Sensing for Resource Management* (C.J. Johannsen and J.L. Sanders, editors), Soil Conservation Society of America, Ankney, Iowa, pp. 317-328.

Alföldi, T.T., and J.C. Munday, 1978. Water quality analysis by digital chromaticity mapping of Landsat data, *Canadian Journal of Remote Sensing*, 4(2):108-126.

Bartolucci, L. A., B.F. Robinson, and L.F. Silva, 1977. Field measurements of the spectral response of natural waters, *Photogrammetric Engineering & Remote Sensing*, 43(5):595-598.

Bhargava, D.S., and D.W. Mariam, 1990. Spectral reflectance relationships to turbidity generated by different clay materials, *Photogrammetric Engineering & Remote Sensing*, 56(2):225-229.

Brown, L.R., 1984. The global loss of topsoil, *Journal of Soil and Water Conservation*, 39:162-165.

Bukata, R.P., J.E. Bruton, and J.H. Jerome, 1985. *Application of Direct Measurements of Optical Parameters to the Estimation of Lake Water Indicators*, Environment Canada IWD Scientific Series No. 140.

Bukata, R.P., J.H. Jerome, K.Y. Kondratyev, and D.V. Pozdnyakov, 1991. Estimation of organic and inorganic matter in inland waters: optical cross sections of lakes Ontario and Ladoga, *Journal of Great Lakes Research*, 17(4):461-469.

Campbell, J.B., 1987. *Introduction to Remote Sensing*, The Guilford Press, New York, pp. 404-432.

Curran, P.J., and E.M.M. Novo, 1988. The relationship between suspended sediment concentration and remotely sensed spectral radiance: a review. *Journal of Costal Research*, 4(3):351-368

Deering, D. W., 1989. Field measurements of bidirectional reflectance, *Theory and Applications of Optical Remote Sensing*, (G. Asar, editor), John Wiley & Sons, New York, pp. 14-61.

Figure 10. Correlation between SSC and first derivative at 823.3 nm.
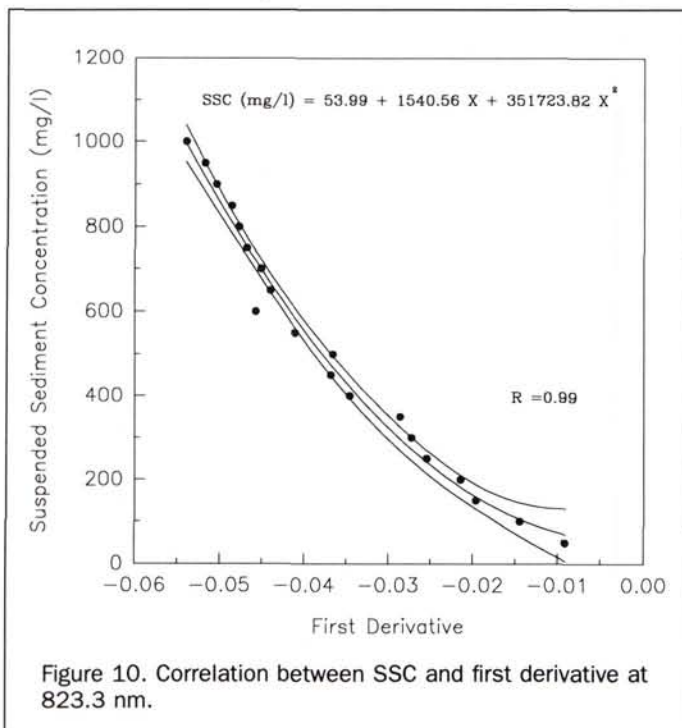
Dekker, A.G., T.J. Malthus, and E. Seyhan, 1992. The effect of spectral bandwidth and positioning on the spectral signature analysis of inland waters, *Remote Sensing of Environment*, 41: 211-225.

Demetriades-Shah, T.H., M.D. Steven, and J.A. Clark, 1990. High resolution derivative spectra in remote sensing, *Remote Sensing of Environment*, 33:55-64.

Doerffer, R., J. Fisher, M. Stossel, and C. Brockmann, 1989. Analysis of thematic mapper data for studying the suspended matter distribution in the coastal area of the german bight (North Sea), *Remote Sensing of Environment*, 28:61-73.

Hilton, J., 1984. Airborne remote sensing for freshwater and estuarine monitoring, *Water Resources*, 18(10):1195-1223.

Jensen, J. R., B. Kjerfve, E.W. Ramsey, K.E. Magill, C. Medeiros, and J. Sneed, 1989. Remote sensing and numerical modeling of suspended sediment in Laguna de Terminos, Campeche, Mexico, *Remote Sensing of Environment*, 28:33-44.

Johnson, R. W., 1975. Quantitative suspended sediment mapping using aircraft multispectral data, *Proceedings of NASA Earth Resources Survey Symposium*, Houston, Texas, pp. 2981-2998.

Khorram, S., and H.M. Cheshire, 1985. Remote sensing of water quality in the Neuse River Estuary, North Carolina, *Photogrammetric Engineering & Remote Sensing*, 54:329-341.

Lathrop, R. G., Jr., and T.M. Lillesand, 1989. Monitoring water quality and river plume transport in Green Bay, Lake Michigan with SPOT-1 Imagery. *Photogrammetric Engineering & Remote Sensing*, 55:349-354.

Lillesand, T. M., and R.W. Kiefer, 1987. *Remote Sensing and Image Interpretation, 2nd Edition*, John Wiley & Sons, New York, pp. 1-34.

Lyon, J. G., K.W. Bedford, Chieh-Cheng.J. Yen., D.H. Lee, and D.J. Mark, 1988. Determinations of suspended sediment concentration from Multiple day Landsat and AVHRR data, *Remote Sensing of Environment*, 25:107-115.

McCluney, W. R., 1976. Remote measurement of water color, *Remote Sensing of Environment*, 5:3-33.

McKim, H. L., C.J. Merry, and R.W. Layman, 1984. Water quality monitoring using airborne spectroradiometer, *Photogrammetric Engineering & Remote Sensing*, 50:353-360.

Montovani, J. E., and A.P. Cabral, 1992. Tank depth determination for water radiometric measurements, *International Journal of Remote Sensing*, 14:2727-2733.

Moore, G. K., 1978. Satellite surveillance of physical water quality characteristics, *Proceedings of the Twelfth International Symposium on Remote Sensing of Environment*, Environmental Research Institute of Michigan, Ann Arbor, Michigan, pp. 445-462. Munday, J. C., and T.T. Alföldi, 1979. Landsat test of diffuse reflectance models for aquatic suspended solids measurement, *Remote Sensing of Environment*, 8:169-183.

Novo, E.M.L.M., J.D. Hansom, and P.J. Curran, 1989a. The effect of sediment type on the relationship between reflectance and suspended sediment concentration, *International Journal of Remote sensing*, 10:1283-1289.

———, 1989b. The effect of viewing geometry and wavelength on the relationship between reflectance and suspended sediment concentration, *International Journal of Remote Sensing*, 10:1357-1372.

Novo, E. M. L. M., C.A. Stefen, and C.A. Braga, 1991. Results of a laboratory experiment of relating spectral reflectance to total suspended solids, *Remote Sensing of Environment*, 36:67-72.

Quibell, G., 1991. The effect of suspended sediment on reflectance from freshwater algae, *International Journal of Remote Sensing*, 12:177-182.

Ritchie, J.C., F.R. Schiebe, R.B. Wilson, and J. May, 1975. Sun angle, reflected solar radiation and suspended sediments in North Mississippi reservoirs, *Remote Sensing of Earth Resources* (F. Shahrokhi, editor), University of Tennessee, Tullahoma, Tennessee, pp. 555-564.

Ritchie, J.C., F.R. Schiebe, and J.R. Mchenry, 1976. Remote sensing of suspended sediments in surface waters, *Photogrammetric Engineering & Remote Sensing*, 42:1539-1545.

Ritchie, J.C., C.M. Copper, and F.R. Schiebe, 1990. The relationship of MSS and TM data with suspended sediments, chlorophyll, and temperature in Moon Lake, Mississippi, *Remote Sensing of Environment*, 33:137-148.

Schiebe, F. R., J.A. Harrington, and J.C. Ritchie, 1992. Remote sensing of suspended sediments: the Lake Chicot, Arkansas project, *International Journal of Remote Sensing*, 13:1478-1509.

Vertucci, F. A., and G.E. Likens, 1989. Spectral reflectance and water quality of Adirondack mountain region lakes, *Limnology and Oceanography*, 34:1656-1672.

Luoheng Han

Luoheng Han received his M.S. in Geography from Northeast Normal University (NENU), P. R. China, in 1985. From August 1985 to August 1988, he was employed as Lecturer in the Department of Geography, NENU. He is currently working toward his Ph.D. in Geography at the University of Nebraska, specializing in remote sensing and water resources.

Donald C. Rundquist

Donald C. Rundquist is a Professor with the Conservation and Survey Division, Institute of Agriculature and Natural Resources, University of Nebraska-Lincoln. He also serves ad Director of the Center for Advanced Land Management Information Technologies (CALMIT), and holds adjunct appointments in Agricultural Meteorology, Agronomy, Geography, and Geology.